Selective Carbonyl Insertion and Ethene Hydroformylation on a $[Ru_6C(CO)_{16}Me]^-$–SiO_2 Catalyst

Yasuo Izumi,[*,†,a] **Teiji Chihara,**[b] **Hiroshi Yamazaki**[b] **and Yasuhiro Iwasawa**[*,a]
[a] *Department of Chemistry, School of Science, The University of Tokyo, Hongo, Bunkyo-ku, Tokyo 113, Japan*
[b] *The Institute of Physical and Chemical Research, Wako-shi, Saitama 351-01, Japan*

Stoichiometric acetaldehyde formation by insertion of CO into the methyl ligand and catalytic ethene hydroformylation on the cluster, $[Ru_6C(CO)_{16}Me]^-$ supported on silica at 373–473 K have been investigated to understand the effects of the catalysis on the metal cluster framework and also to develop new catalytic systems on a molecular scale. Two elementary steps for stoichiometric acetaldehyde formation, (*i*) from methyl to acetyl and (*ii*) from acetyl to acetaldehyde, were observed by Fourier-transform IR spectroscopy. The rate of (*i*) in CO + H_2 was faster than that in CO, suggesting a hydride-promoted mechanism for carbonyl insertion (acetyl formation). The hydride promotion and hydrogen pressure dependence suggested dissociative adsorption of H_2 so as to bridge a Ru-Ru and the incorporation of the multi-Ru sites in the acetaldehyde formation mechanism. The reductive elimination of hydride and methyl ligands upon methane formation was much slower than the reductive elimination of H and MeO for acetaldehyde formation as well as the insertion of CO (methyl migration) for acetyl formation. In terms of this specific feature the catalytic hydroformylation of ethene was found to proceed on the catalyst with nearly 100% selectivity at 398 K in the case of highly dehydrated SiO_2 (823 K). The retention of the cluster framework under the reaction conditions was confirmed by extended X-ray adsorption fine structure curve-fitting analysis. On the contrary, $[Ru_6C(CO)_{16}Me]^-$ in a homogeneous system did not catalyse this reaction and conventional impregnation Ru–SiO_2 catalysts showed only 0–0.09% selectivities. A reaction mechanism is presented.

Metal clusters have been utilized as precursors of dispersed metal particles on supports or as well defined models of adsorption structures on metal catalysts, or as good examples for mechanistic research. The structure and stability of supported metal clusters have been extensively studied.[1] For example, $[Ru_3(CO)_{12}]$ has been demonstrated to react with Al_2O_3 to form $[Ru_3(CO)_{10}(\mu\text{-H})(\mu\text{-OAl})]$ at room temperature,[2,3] while under CO–H_2 the clusters $[Ru_3(CO)_{12}]$ or $[Re_3H_3(CO)_{12}]$ on oxide surfaces often exhibit metal aggregation or metal–metal bond cleavage, depending on the ambient gases.[4,5] The behaviours of $[Rh_4(CO)_{12}]$ and $[Rh_6(CO)_{16}]$ on various oxides have also been examined by many workers; a reversible transformation of the structures between $Rh_6(CO)_{16-m}$ and $Rh(CO)_2$ occurs.[1] These varying transformations of the metal framework of precursor clusters to ill defined metal species or particles make it difficult to observe the relation between the cluster structure and the reactivity or the catalytic performance, and also to explore the catalytic reaction mechanism on a molecular scale.

While the hydroformylation of alkenes or carbon monoxide insertion reactions occur in principle on mononuclear metal complexes in homogeneous systems, supported metal catalysts show a maximum activity at an optimum metal particle size.[6] This implies that, in heterogeneous systems, metal clusters or ensembles are more active than are single-metal sites, suggesting an important role of metal–metal frameworks.

The aim of the present study was to develop a new catalytic system with appropriate metal–metal bonding for hydroformylation. We chose a ruthenium carbidocarbonyl cluster, $[Ru_6C(CO)_{16}Me]^-$, which has a more stable metal framework than those of $[Ru_3(CO)_{12}]$ and $[Ru_6(CO)_{18}]^{2-}$ under the catalytic reaction conditions.[7] Analysis of Ru–Ru and multiple scattering Ru(–C–)Ru peaks by EXAFS (extended X-ray absorption fine structure) has shown[8] that $[Ru_6C(CO)_{16}Me]^-$ supported on silica has the same octahedral structure as that of the precursor. Furthermore, the cluster $[Ru_6C(CO)_{16}Me]^-$ with an alkyl ligand besides CO ligands was regarded as a good precursor to examine the elementary step of hydroformylation. The supported ruthenium cluster can be characterized easily by EXAFS and Fourier-transform infrared spectroscopy by comparison with the precursor itself. Another aim was to determine the physical and chemical (electronic) effects of the carbido-carbon as a four-electron donor on the catalytic properties.

The cluster $[Ru_6C(CO)_{16}Me]^-$ was converted into $[Ru_6C(CO)_{16}(COMe)]^-$ by heating and characterized by X-ray diffraction.[7] However, the hydrogenation of $[Ru_6C(CO)_{16}(COMe)]^-$ to form acetaldehyde never proceeds in a homogeneous system. Rather, $[Ru_6C(CO)_{16}(COMe)]^-$ is decomposed to methane by the reverse reaction.[9] In the present article a new possibility for $[Ru_6C(CO)_{16}Me]^-$ supported on silica is reported. The mechanism for stoichiometric formation of acetaldehyde from the methyl ligand and highly selective catalysis for ethane hydroformylation are discussed.

Experimental

Catalyst Preparation.—Silica was pretreated at 473 or 823 K before use as a support. The salt $[NMe_3(CH_2Ph)][Ru_6C(CO)_{16}Me]$ (Fig. 1) was supported on SiO_2 by immersion of the SiO_2 into a CH_2Cl_2 solution of the cluster for 1 h, followed by removal of the solvent under vacuum.[8] The samples prepared by using the silica treated at 473 and 823 K are denoted catalysts **1** and **2**. Results given without special notation are for catalyst **1**. Conventional impregnation ruthenium catalysts as references were prepared from aqueous solutions of $[Ru(NO)(NO_3)_3]$ (N.E. Chemcat. Co.) or $RuCl_3 \cdot 3H_2O$ (Nakarai Tesque Co.). The loading of ruthenium catalyst

---

† *Present address:* Department of Environmental Chemistry and Engineering, Tokyo Institute of Technology, Nagatsuta, Midori-ku, Yokohama 227, Japan.

Table 1 Rates of each reaction step

	Rate/min^{-1}				
Step	373	398	423	473 K	E_a/kJ mol^{-1}
CO + H_2^{a}					
CO + Me $\longrightarrow$ MeCO^b	—	(0.018_2)	(0.034_2)	—	—
MeCO + $\frac{1}{2}H_2$ $\longrightarrow$ MeCHO(g)^b	—	0.09_7	0.12_1	—	—
CO + Me + $\frac{1}{2}H_2$ $\longrightarrow$ MeCHO(g)	0.0096_3	0.018_2	0.034_2	0.089_1	32.3
Me + $\frac{1}{2}H_2$ $\longrightarrow$ CH_4(g)	0	0.0029_1	0.010_1	0	72.6
MeCHO selectivity (%)^c	100	86	77	100	—
CO^d					
CO + Me $\longrightarrow$ MeCO^b	—	0.010_1	0.011_1	—	—
MeCO + OH $\longrightarrow$ MeCHO(g) + O(s)^b	—	(0.0045_5)	(0.009_1)	—	—
CO + Me + OH $\longrightarrow$ MeCHO(g) + O(s)	0.0020_2	0.0045_5	0.009_1	0.029_4	38.7
Me + OH $\longrightarrow$ CH_4(g) + O(s)	0.0002_1	0.0008_2	0.003_1	0.029_5	75.3
MeCHO selectivity (%)^c	90	86	75	50	—
H_2^{e}					
CO + Me + $\frac{1}{2}H_2$ $\longrightarrow$ MeCHO(g)	0.0064_1	0.019_1	0.051_1	—	54.8
Me + $\frac{1}{2}H_2$ $\longrightarrow$ CH_4(g)	0.007_1	0.03_1	0.09_1	—	70.0
MeCHO selectivity (%)^c	48	39	36	—	—
In vacuum					
CO + Me + OH $\longrightarrow$ MeCHO(g) + O(s)	0	0	—	—	—
Me + OH $\longrightarrow$ CH_4(g) + O(s)	0.0090_1	0.077_3	—	—	104
MeCHO selectivity (%)^c	0	0	—	—	—
Carbonyl exchange^f					
Terminal CO $\longrightarrow$ CO(g)^b	0.080	0.17	0.44	—	40.2
Bridging CO $\longrightarrow$ CO(g)^b	0.083	0.16	0.42	—	39.0

The reaction rates were normalized to the amount of supported cluster. Values in parentheses were postulated to be equal to the rate of acetaldehyde formation because that step was rate determining. The rates were measured in the initial stage of reaction. [a] 13 kPa CO, 3.3 kPa H_2. [b] Estimated from IR observations. [c] $100 \times r_{MeCHO}/(r_{MeCHO} + r_{CH_4})$%. [d] 13 kPa CO. [e] 13 kPa H_2. [f] 8.0 kPa CO.

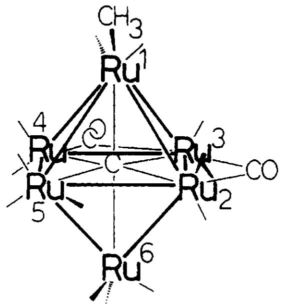

Fig. 1 The crystal structure of $[Ru_6C(CO)_{16}Me]^-$ (ref. 7)

was 3% by weight. The samples impregnated from ruthenium salts were dried at 383 K for 1 h and calcined at 673 K. They were again oxidized with O_2, followed by reduction with H_2 at 673 or 823 K *in situ* before catalytic reaction.

Gas Desorption and Catalytic Reaction.—Methane evolution from the methyl ligand was monitored by a gas chromatograph using a column of 5A molecular sieves (2 m) at 353 K, and acetaldehyde and methanol formed during the stoichiometric reaction of ligands were also analysed by using a column of dioctyl sebacate (4 m) at 353 K. The $[Ru_6C(CO)_{16}Me]^-$–SiO_2 remaining after stoichiometric acetaldehyde formation in CO (13 kPa) and H_2 (3.3 kPa) for 55 min at 398 K was cooled rapidly ($\approx$30 s) and evacuated at 293 K for 1 min, then the temperature-programmed desorption (TPD) spectrum was measured between 293 and 673 K at a heating rate of 4 K min^{-1}. The gases H_2, HD and D_2 were monitored by mass spectrometry. The TPD for intact $[Ru_6C(CO)_{16}Me]^-$–SiO_2 was also measured as a control. In catalytic ethene hydroformylation in a closed circulating system, ethene and ethane were analysed by a VZ-10 column (2 m), and propanal and propanol by a dioctyl sebacate column at 353 K.

Infrared Spectroscopy.—Silica (0.06 g) was pressed to a disk and placed in an IR cell equipped with two NaCl windows and attached to a closed circulation system. The silica disk was treated at 473 K under vacuum. A methanol solution of $[Ru_6C(CO)_{16}Me]^-$ was dropped on to the silica disk by use of a glass capillary in a high-purity argon (99.9999%) atmosphere.

Results

Stoichiometric Acetaldehyde Formation.—The initial rates for the formation of acetaldehyde or methane in CO + H_2, CO, H_2 and vacuum are listed in Table 1. The rates are normalized to the amount of $[Ru_6C(CO)_{16}Me]^-$. The selectivity for the formation of acetaldehyde by the reaction between methyl and carbonyl ligands followed by the reduction with H_2 was high: 77–100% in CO + H_2 at 373–473 K (Table 1). In contrast no acetaldyhyde was formed in vacuum, where only CH_4 was formed by the reaction of the methyl ligand with the OH groups (Table 1). However, acetaldehyde was also formed in the presence of H_2 alone (Table 1), suggesting that H_2, not OH, reacts with an acetyl intermediate. Acetaldehyde formation with CO + CH_3 + OH (in vacuum or CO) was much less favourable than that with CO + CH_3 + H_2 (in H_2 or CO + H_2). The reaction of the methyl ligand with OH (reaction in vacuum) was remarkably suppressed by the presence of CO (reaction in CO) as shown in Table 1. The activation energies for each step are also given in Table 1.

The dependence of the rate of acetaldehyde formation on hydrogen pressure (P_{H_2}) was measured in the range 0–41 kPa at

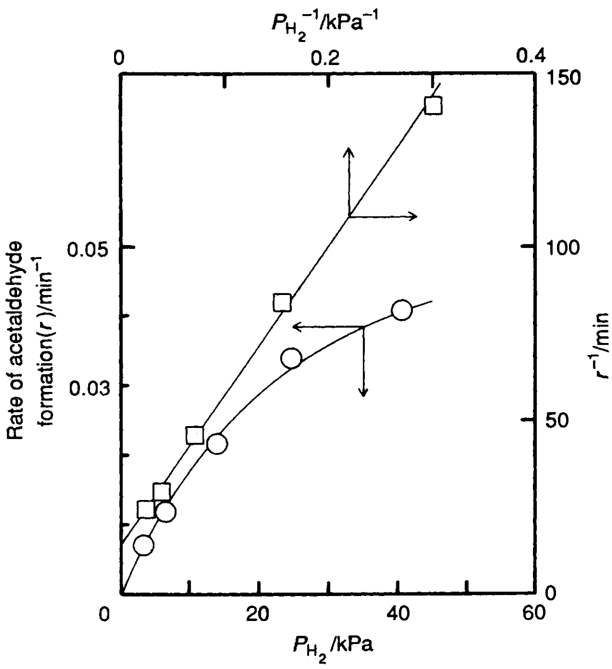

Fig. 2 Hydrogen pressure dependence of the rate of acetaldehyde formation on $[Ru_6C(CO)_{16}Me]^-$–SiO_2 in CO (13 kPa) + H_2 (3.3–41 kPa) at 398 K

a constant P_{CO} of 13 kPa. The rate at 398 K showed an upward curvature (Fig. 2).

In Situ Observation of the Reaction Steps to Acetaldehyde Formation by Fourier-transform IR Spectroscopy.—Fig. 3 shows the IR spectra for the incipient supported cluster (*a*), and for the samples after reaction in CO + H_2 at 448 (*b*) and 473 K (*c*). The peaks were deconvoluted by Gaussian curve-fitting techniques. The analysis was always performed with the deconvoluted peaks. The incipient supported cluster had a peak pattern [2074w, 2034s, 1986m and1768m(br) cm^{-1}] similar to that for the unsupported cluster [2074w, 2020s, 1960m and 1808m(br) cm^{-1}].[8] A main peak for terminal CO is observed at 2034 cm^{-1}. The peak for bridging CO (Fig. 1) appears at 1768 cm^{-1} in Fig. 3. The peak at 1986 cm^{-1} became relatively strong upon heating at 473 K in CO + H_2 as compared with the peak for the incipient supported cluster, as shown in Fig. 3, while the intensity of the bridging carbonyl peak at 1768 cm^{-1} increased a little.

The IR spectra for the supported cluster heated under CO + H_2 are shown in Fig. 4. No new peak corresponding to acetyl was observed, suggesting that the formation of acetyl by insertion of CO into methyl is slower than the subsequent reaction of the acetyl with H_2 to form acetaldehyde. Hence, we postulate that the rate of acetyl formation is equal to the observed overall rate for acetaldehyde formation in Table 1. The spectra in Fig. 4 were deconvoluted and the intensities of each peak are plotted against the reaction time at 398, 423, 448 and 473 K in Fig. 5. Accompanying the formation of acetaldehyde, the peak at 2034 cm^{-1} decreased and that at 1988 cm^{-1} developed at temperatures higher than 423 K. The intensity of the peak for bridging CO at 1768 cm^{-1} was reduced but recovered at 473 K. The acetaldehyde produced seems to be desorbed very rapidly and trapped in a U-shaped tube in liquid nitrogen, no peaks being ascribable to it in Fig. 4.

Upon heating the $[Ru_6C(CO)_{16}Me]^-$–SiO_2 under 13 kPa CO without H_2, a new peak at 1608 cm^{-1} appeared [Fig. 6(*b*)–(*e*)]. In the case of the ^{13}CO-exchanged cluster a peak at 1570 cm^{-1} was observed. When the surface cluster showing a peak at 1570 cm^{-1} was reduced with H_2 at 423 K acetaldehyde was formed accompanied with a decrease in the intensity of the 1570

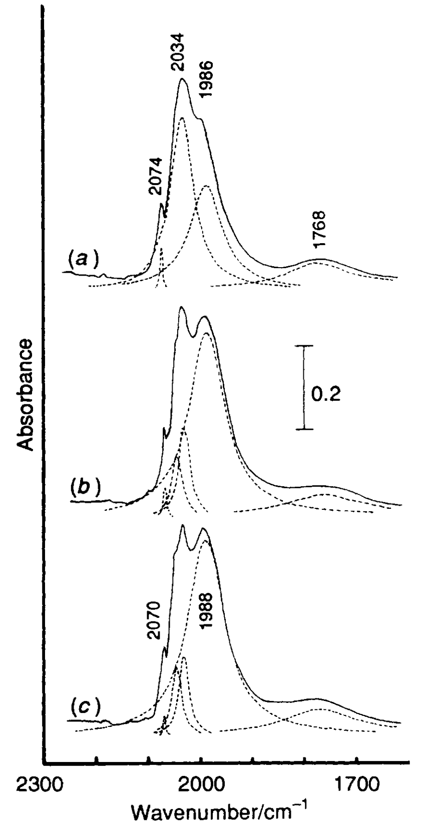

Fig. 3 Peak deconvolutions of IR spectra of untreated (incipient) $[Ru_6C(CO)_{16}Me]^-$–SiO_2 (*a*), $[Ru_6C(CO)_{16}Me]^-$–SiO_2 in CO (13 kPa) + H_2 (3.3 kPa) for 5.5 min at 448 K (*b*), and $[Ru_6C(CO)_{16}Me]^-$–SiO_2 in CO (13 kPa) + H_2 (3.3 kPa) for 6.5 min at 473 K (*c*)

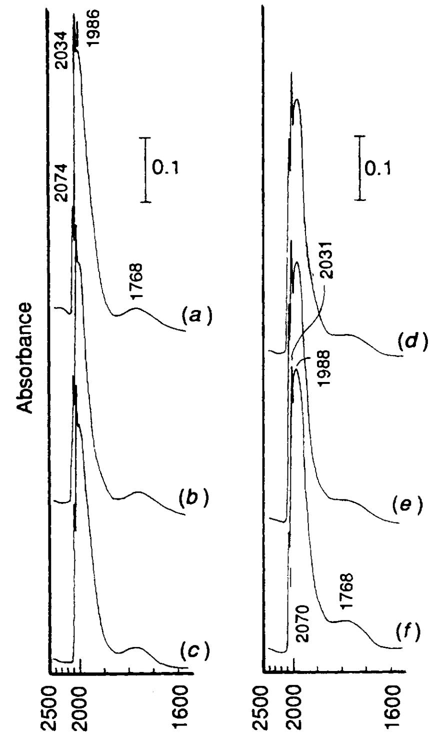

Fig. 4 The change in IR spectra of $[Ru_6C(CO)_{16}Me]^-$–SiO_2 in CO (13 kPa) + H_2 (3.3 kPa) in the ν(CO) region at (*a*) 323 K, (*b*) 373 K, (*c*) 398 K for 14.5 min, (*d*) 423 K for 27.5 min, (*e*) 448 K for 0.5 min (*f*) 473 K for 6.5 min

cm^{-1} peak. These results indicate that the peak at 1608 cm^{-1} (1570 cm^{-1}) is due to acetyl. For the quantitative estimation of the rates of formation and reaction of the acetyl from the IR absorbance, 0.06 g of 3% $[Ru_6C(CO)_{16}Me]^-$–SiO_2 was pressed as rapidly as possible (the precursor is stable in air) and the increase or decrease in the intensity of the acetyl peak under different conditions was correlated with the amount of acetaldehyde formed. To determine the rate of the acetyl hydrogenation step with H_2, we first observed the IR spectrum in CO and switched the ambient CO to a mixture of CO + H_2 very rapidly, followed by observation of the decrease in the acetyl peak at 398 or 423 K (Fig. 7). The rate of the acetyl hydrogenation was estimated from the initial decrease in the acetyl peak after the switch of the ambient gas from CO to CO + H_2. The results are listed in Table 1. The acetyl peak in CO was augmented at 398 K in region I of Fig. 7. This augmentation means that the hydrogenation of acetyl by surface OH groups is slow, and hence the overall rate of acetaldehyde formation is suggested to be approximately equal to the rate of acetyl hydrogenation in CO. The rates of acetaldehyde formation in CO are shown in Table 1. The carbonyl insertion step in CO + H_2 was twice as fast at 398 K (0.018 *vs* 0.010 min^{-1}) and three times as fast at 423 K (0.034 *vs.*

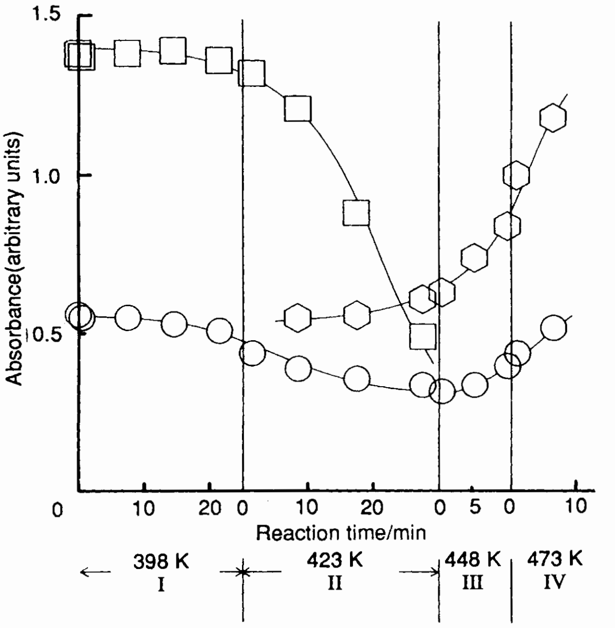

Fig. 5 The change in relative intensity of IR peaks at 2634 (□), 1988 (⬡) and 1768 cm^{-1} (○) for $[Ru_6C(CO)_{16}Me]^-$–SiO_2 in CO (13 kPa) + H_2 (3.3 kPa) at 398, 423, 448 and 473 K

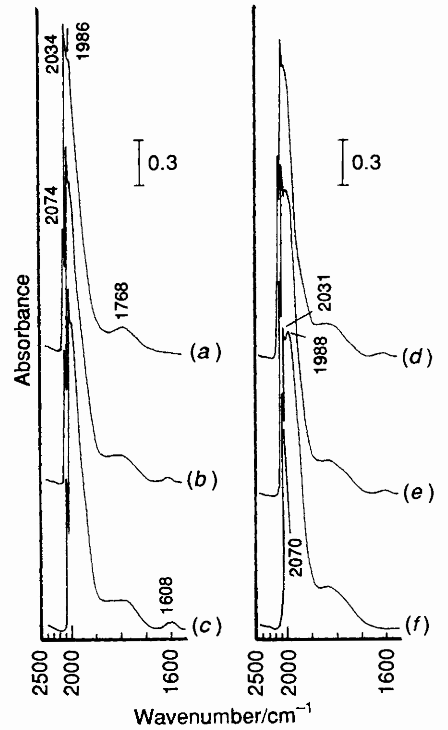

Fig. 6 The change in IR spectra of $[Ru_6C(CO)_{16}Me]^-$–SiO_2 in CO (13 kPa) or in CO (13 kPa) + H_2 (3.3 kPa) in the ν(CO) region at (*a*) 323 K in CO, (*b*) 398 K for 0.5 min in CO, (*c*) 398 K for 5.5 min in CO, (*d*) 423 K for 11.0 min in CO, (*e*) 423 K for 0.5 min in CO + H_2, and (*f*) 423 K for 16.5 min in CO + H_2

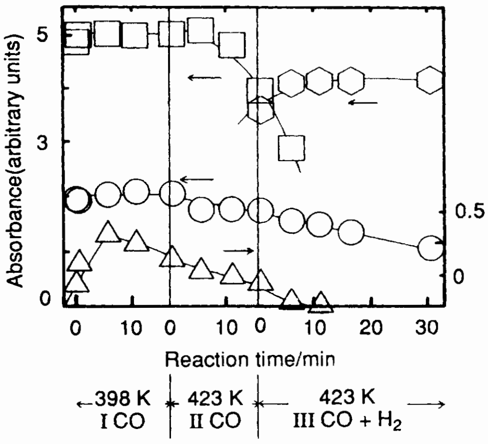

Fig. 7 The relative intensity of IR peaks at 2034 (□), 1988 (⬡), 1768 (○) and 1608 cm^{-1} (△) for $[Ru_6C(CO)_{16}Me]^-$–SiO_2 in CO (13 kPa) or in CO (13 kPa) + H_2 (3.3 kPa) at 398 and 423 K; *t* = 0 min in region I is the time that the temperature reached 398 K upon rapid heating from room temperature

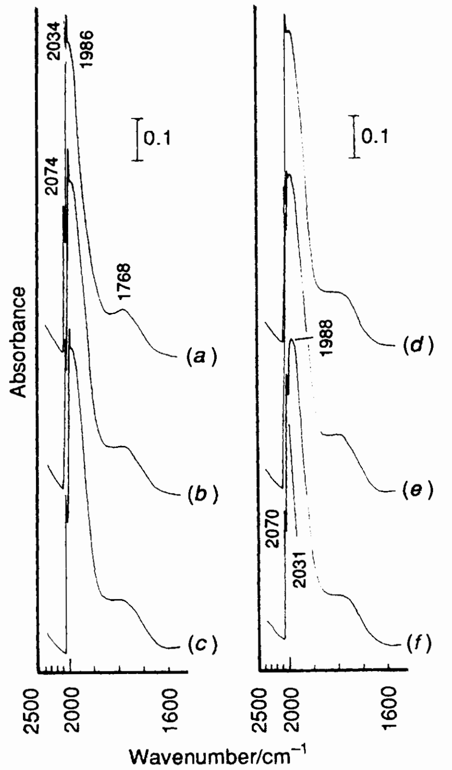

Fig. 8 The change in IR spectra of $[Ru_6C(CO)_{16}Me]^-$–SiO_2 in vacuum in the ν(CO) region at (*a*) 373 K, (*b*) 423 K for 5.5 min, (*c*) 448 K for 5.0 min, (*d*) 473 K for 6.5 min, (*e*) 498 K for 5.5 min, and (*f*) 498 K for 6.5 min

0.011 min^{-1}) than that in CO. This indicates that the insertion was enhanced by the presence of H_2.

The changes in the IR peaks in vacuum was also measured (Fig. 8). The terminal CO shifted from 2034 to 1988 cm^{-1} upon heating to 473 K. In contrast to the case of CO + H_2, the acetyl peak was not observed, which is in accord with no acetaldehyde formation from the methyl and carbonyl ligands in vacuum at any temperature (Table 1). The intensity of the peak at 2034 cm^{-1} decreased at 423 K and the peaks at 1988 and 1768 cm^{-1} also decreased as shown in Fig. 9. These results agree with the lower stability of the cluster framework in vacuum as demonstrated by EXAFS [co-ordination numbers $N_{\text{Ru–Ru}}$ and $N_{\text{Ru(–C–)Ru}}$ were reduced to 2.8 (d = 0.288 nm) and 0.8 (d = 0.410 nm) from 4.0 (d = 0.290 nm) and 1.0 (d = 0.410 nm) at 423 K, respectively].[8]

We also determined the rate of the exchange reaction between gas-phase ^{13}CO and ligand CO by monitoring the peak shift of terminal CO (2034 to 1984 cm^{-1}) and bridging CO (1768 to 1720 cm^{-1}) (Table 1). The exchange rates for terminal and bridging CO were the same at each reaction temperature and much faster than the rates of acetaldehyde or methane formation.

TPD Measurements.—One of the two H atoms of H_2 should remain on the ruthenium cluster framework after the acetaldehyde formation with CO + Me + H_2. The TPD spectrum after stoichiometric acetaldehyde formation for 55 min at 398 K in CO + D_2 showed a peak for hydrogen desorption [H_2 (main) and HD] at 473 K [Fig. 10(*a*)]. The TPD spectrum of $[Ru_6C(CO)_{16}Me]^-$–SiO_2 without treatment under CO + D_2 showed no desorption of hydrogen/deuterium [Fig. 10(*b*)]. The H_2 produced may be derived from the exchange of D on Ru_6 with surface OH groups before recombination and desorption.

Catalytic Ethene Hydroformylation.—As the SiO_2-supported $[Ru_6C(CO)_{16}Me]^-$ cluster selectively formed acetaldehyde at 373–473 K under a mixture of CO + H_2 as shown in Table 1, a vacant site on the cluster framework can be obtained by stoichiometric carbonyl insertion (methyl migration) reaction in CO + H_2 at 398 K. Thus it was expected that the cluster obtained *in situ* would be active and selective for catalytic ethene hydroformylation involving a carbonyl-insertion step. A high ratio of ethene pressure (17.3 kPa) to CO pressure (3.3 kPa) was chosen for efficient formation of ethyl species. The steady-state activity and selectivity are shown in Table 2. The supported cluster catalysts were not deactivated for more than 36 h at 398 K. The best selectivity (12%) to propanal + propanol on catalyst **1** was observed at 433 K. On the contrary, impregnation Ru–SiO_2 catalysts prepared from $RuCl_3·3H_2O$ or $[Ru(NO)(NO_3)_3]$ showed low selectivities (0–0.09%) under identical reaction conditions (Table 2). The conventional impregnation catalysts cannot produce the hydroformylation products selectively even if the total activity of the impregnation catalysts is as much as that of the supported carbido-cluster catalysts.

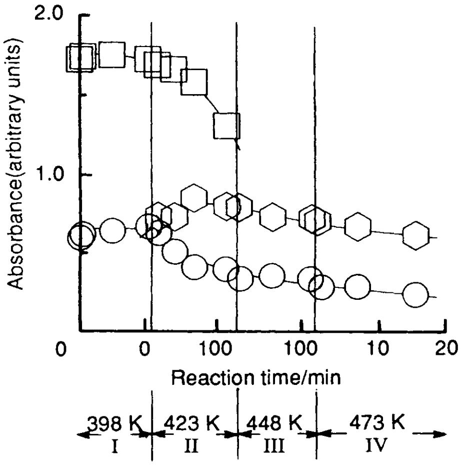

Fig. 9 The change in relative intensity of the IR peaks of $[Ru_6C(CO)_{16}Me]^-$–SiO_2 in vacuum at 398, 423, 448 and 473 K. Peaks as in Fig. 5.

The $[Ru_6C(CO)_{16}Me]^-$ supported on silica pretreated at 823 K (catalyst **2**) was found catalytically to produce propanal with 100% selectivity at 398 K (Table 2). In TPD experiments the selective formation of acetaldehyde (82%) was observed with this catalyst, similar to the result for catalyst **1** (77%) given in our previous paper.[8]

Discussion

It was found that the reaction of methyl and carbonyl ligands to form acetaldehyde selectively proceeded on $[Ru_6C(CO)_{16}Me]^-$–SiO_2 under CO + H_2 (Table 1), while no formation of acetaldehyde has been observed with $[Ru_6C(CO)_{16}Me]^-$ in solution.[7,9] Detailed EXAFS analysis of the supported cluster

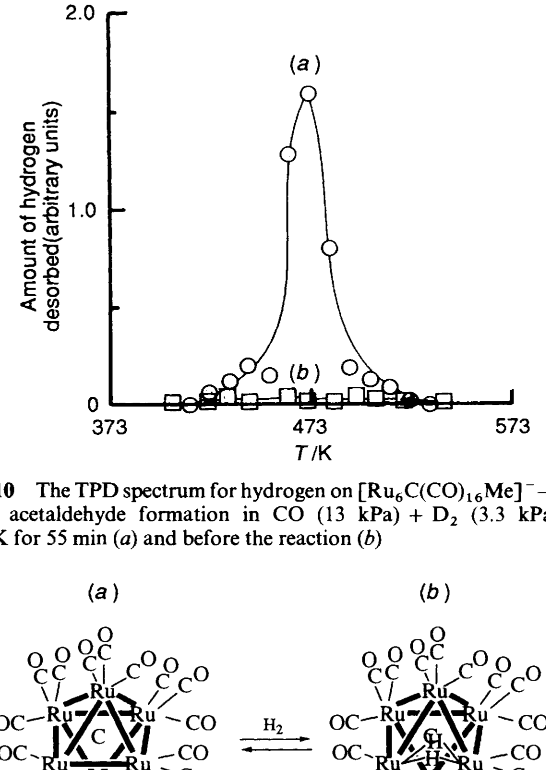

Fig. 10 The TPD spectrum for hydrogen on $[Ru_6C(CO)_{16}Me]^-$–SiO_2 after acetaldehyde formation in CO (13 kPa) + D_2 (3.3 kPa) at 398 K for 55 min (*a*) and before the reaction (*b*)

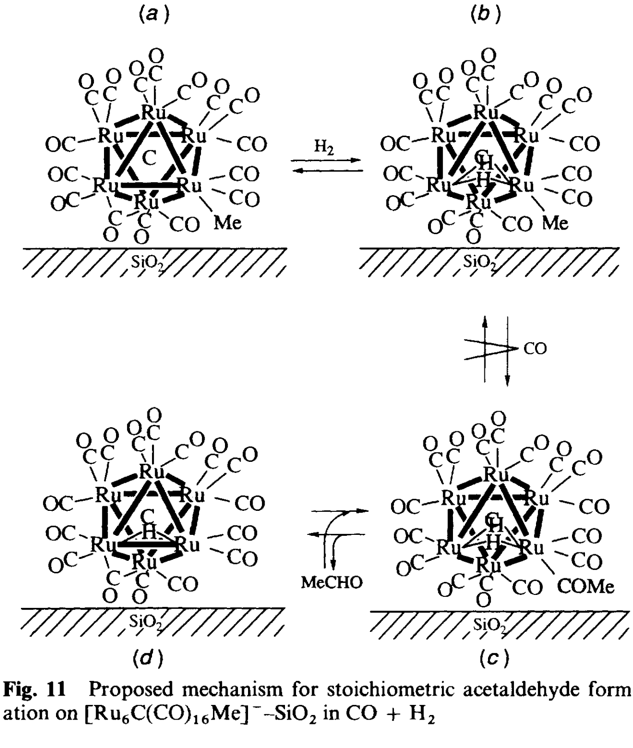

Fig. 11 Proposed mechanism for stoichiometric acetaldehyde formation on $[Ru_6C(CO)_{16}Me]^-$–SiO_2 in CO + H_2

Table 2 Steady-state activity and selectivity of the cluster catalysis and impregnation catalysts for catalytic ethene hydroformylation

		TOF/10^{-3} min^{-1}			
Catalyst	T/K	Ethane	Propanal	Propanol	Selectivity (%)
1[a,b]	398	2.3	0.040	0	1.7
	433	14	1.6	0.30	12
2[a,c]	398	0	0.32	0	100
	423	15	2.7	0.41	17
Ru–SiO_2 from $[Ru(NO)(NO_3)_3]$[d]					
	398	110	0	0	0
	433	520	0.088	0	0.02
Ru–SiO from $RuCl_3{\cdot}3H_2O$[d]					
	398	490	0.21	0.22	0.09

Pressure of gases: C_2H_4, 17.3; CO, 3.3; H_2, 10.6 kPa. [a] TOF is defined as the reaction rate per $[Ru_6C(CO)_{16}Me]^-$ cluster. [b] Catalyst prepared from SiO_2 pretreated at 473 K. [c] Catalyst prepared from SiO_2 pretreated at 823 K. [d] TOF is defined as the reaction rate per surface Ru atom.

[for Ru–C, Ru–Ru, Ru(–C–)O, and Ru(–C–)Ru bonds)] demonstrated the stability of the cluster framework under CO or CO + H_2 up to 473 K.[8] The TPD and IR studies revealed that the cluster is physisorbed on silica at 293–373 K,[8] retaining the structure shown in Fig. 11(*a*), where the terminal and bridging CO groups interact with the SiO_2 surface according to the IR peak shifts for both these groups. No CO desorbs at 398 K and hence the co-ordination sphere of the supported cluster is saturated during the stoichiometric reaction of the methyl ligand. Thus H_2 may adsorb dissociatively with cleavage of a Ru–Ru bond as shown in Fig. 11(*b*) (see later). No acetaldehyde was formed in vacuum over $[Ru_6C(CO)_{16}Me]^-$–SiO_2 implying that gas-phase CO is necessary for this reaction. Besides the usual effect of CO, hydrogen promoted the insertion of CO by a factor of 2–3 to form acetyl as shown in Table 1 (comparison of the rates in CO and CO + H_2). The increase in the rate for acetyl formation in CO + H_2 in Table 1 is interpreted to be due to the total effects of CO and H_2.

The hydrogen atoms are shown as bridging in Fig. 11(*b*) for the following reasons. From a knowledge of metal cluster chemistry H atoms prefer to adsorb at bridging sites for ruthenium clusters. The hydrides were not observed by careful Fourier-transform IR measurements. The bridging hydrides may be weak and appear in a low-frequency region. There are several possible sites for adsorption of H_2, *i.e.* bridging between Ru^1 and Ru^2, Ru^1 and Ru^3, Ru^1 and Ru^4, or Ru^1 and Ru^5 (Fig. 1). The intensity of the bridging carbonyl peak decreased by 43% during the course of acetaldehyde formation (Figs. 4 and 5), which may exclude the Ru^1–Ru^4 or Ru^1–Ru^5 sites. The 'carbonyl insertion process' is generally believed to proceed with alkyl migration.[10–14] The fact that the carbonyl insertion was promoted by the hydrides (Table 1) is favourably explained in the case of Ru^1–Ru^2 rather than in the case of Ru^1–Ru^3. Another possible absorption mode is splitting of H_2 at the adjacent bridging sites, *i.e.* Ru^1–Ru^2 and Ru^1–Ru^5. However, this is less plausible because it is difficult to explain the reduction of bridging CO with no desorption of CO from the Ru^1–Ru^5 site. When two hydrogen atoms are adsorbed at the bridging site between Ru^1 and Ru^2 they can equally promote carbonyl insertion (methyl migration). The species in Fig. 11(*b*) must be formed before insertion of CO because of the promotion by adsorbed hydrogen. The equilibrium constant for adsorption of H_2 (formation of hydrides) was determined to be 0.034 kPa^{-1} by assuming a Langmuir plot in Fig. 2. Carbon monoxide also promotes acetyl formation, resulting in occupation of the site on Ru^1 in Fig. 11(*c*). The acetyl is subsequently hydrogenated by one of the neighbouring hydrogen atoms, probably with metal–metal rebonding.[15,16]

Although hydrogenation of the acetyl did not take place in solution,[7,9] it readily proceeded with the SiO_2-supported cluster as shown by IR spectroscopy and gas chromatography. The acetyl cluster is preferably subjected to reductive elimination of acetyl and hydride on the surface. The shift of the peak at 2034 to 1988 cm^{-1} and the development of the latter upon heating the supported cluster are due to the interaction of the cluster with silica and the change in the electronic state of the cluster framework caused by the ligand loss upon acetaldehyde formation. The rate of the hydrogenation of acetyl was 4–5 times larger than that of carbonyl insertion (acetyl formation) in CO + H_2, showing the easy conversion of acetyl into acetaldehyde on the supported cluster (Fig. 11). The rate-determining step for acetaldehyde formation is a carbonyl insertion [Fig. 11(*b*) and 11(*c*)]. The hydride of the species in Fig. 11(*d*) is certainly adsorbed on the cluster as shown by TPD (Fig. 10). The adsorption of molecular hydrogen on the cluster is not possible at the reaction temperatures. The reaction of the acetyl with the hydrides proceeded more than 15 times more rapidly than that of the acetyl with the surface OH groups (Table 1).

A 100% selectivity was achieved for catalytic ethene hydroformylation on the cluster in Fig. 11(*d*) which had been produced after stoichiometric reaction of the methyl ligand (Table 2). Under identical conditions, the usual impregnation Ru–SiO_2 catalysts showed only 0–0.9% selectivity (Table 2). The hydrides reacted more favourably (12–30 times) with acetyl than with Me at 398–423 K. Also the reaction of CO + Me was much faster than that of Me + H_2 in CO + H_2 (Table 1). Thus a high selectivity for the hydroformylation reaction is observed with the $[Ru_6C(CO)_{16}Me]^-$–SiO_2 catalyst. The lower surface hydroxyl concentration of catalyst **2** should be one important factor for the higher ethene hydroformylation selectivity. We have considered the possible role of extraneous water, generated during potential side reactions such as dehydration of propanol, in modifying the state of hydroxylation of the silica support during catalysis. However, we feel that the total amount of propanol generated under our catalytic conditions is too low to result in a significant increase in the surface hydroxyl concentration. For example, in the reaction at 423 K on catalyst **2** it was calculated to require more than 100 h to recover to the level of surface hydroxyl concentration on catalyst **1**. During the catalytic reaction the ruthenium cluster framework is maintained as shown by a previous EXAFS analysis[8] {in CO + H_2 at 473 K, $d_{Ru-Ru} = 0.291$ nm with $N = 3.7$ and $d_{Ru(-C-)Ru} = 0.410$ nm with $N = 1.1$, almost the same distances and co-ordination numbers as in the intact $[Ru_6C(CO)_{16}Me]^-$–SiO_2 catalyst}.

There is a problem as to whether the acetyl is derived from gas-phase or ligand CO. It was, impossible to decide because the exchange between gas-phase ^{13}CO and ligand ^{12}CO was more than eight times faster than acetaldehyde formation (Table 1).

Muetterties and Krause[17] reviewed the catalysis of metal clusters in homogeneous systems, in which it has been demonstrated that hydroformylation on metal cluster catalysts such as $[Rh_6(CO)_{16}]$, $[Ru_4H_4(CO)_{12}]$ or $[Ir_4(CO)_{12}]$ does not require multiple metal sites. In general it has rarely been shown that a catalytic reaction on cluster catalysts really needs a cluster framework. It is also often observed that cluster structures are broken under catalytic reaction conditions. The ruthenium carbido cluster supported on silica surface has been demonstrated to be stable under the reaction conditions, showing neither destruction or aggregation of the cluster framework as already mentioned.[8] In the proposed mechanism of Fig. 11 the Ru^1 and Ru^2 atoms participate in the CO insertion/methyl migration step promoted by the hydrides [Fig. 11(*b*) and (*c*)]. It has been reported that $[Ru_3H(CO)_{11}]^-$ catalyses ethene hydroformylation *via* ethyl formation by the reaction of the bridging hydride with adsorbed ethene.[18] However, no hydrogen-promoted feature was observed with this cluster and in this case the reaction can be interpreted as a monometallic or equivalent process, where the bridging hydride only acts as a reactant. The bridging hydrogen on the Ru^1–Ru^2 site in Fig. 11 appears to promote the carbonyl insertion/methyl migration rather than the reaction with methyl ligand (reductive elimination with alkyl). The detailed mechanism of the hydride promotion is not clear, but it may be due to a partial oxidation of ruthenium atoms by oxidative addition of H_2. Thus the high selectivity for propanal/propanol in catalytic ethene hydroformylation on the $[Ru_6C(CO)_{16}Me]^-$–SiO_2 catalyst is suggested to involve a multimetal effect. The role of the carbido-carbon in ruthenium catalysis has been reported in relation to selective methanol synthesis from CO–H_2 instead of the usual methane formation.[19]

Conclusion

The supported $[Ru_6C(CO)_{16}Me]^-$ cluster stoichiometrically forms methane in vacuum, but produces acetaldehyde *via* acetyl with good selectivities of 75–100% at 378–423 K in CO or CO + H_2, while in solution the cluster forms only methane (never acetaldehyde). The cluster framework was maintained up to 473 K, as shown by the retention of the Ru(–C–)Ru multiple scattering shell by EXAFS. Hydrogen seems to adsorb by bridging the Ru^1–Ru^2 bond. The observation of the H- and CO-promoted acetyl formation suggests the mechanism for acetaldehyde formation on the Ru^1 atom co-ordinated to the methyl ligand (Fig. 11). In this mechanism hydrogen induces cleavage of a Ru–Ru bond and the carbonyl ligand changes from bridging to terminal and upon acetaldehyde formation the cleaved bond is reformed as is the bridging CO, as shown by the IR spectra. A vacant site on the Ru^1 atom of the Ru_6C framework on SiO_2 with less surface hydroxyl concentration (pretreated at 823 K) is created after the stoichiometric acetaldehyde formation, at which catalytic ethene hydroformylation proceeds with 100% selectivity at 398 K, while under identical conditions conventional impregnation Ru–SiO_2 catalysts showed much lower selectivities (0–0.09%).

References

1 *Metal Cluster in Catalysis,* eds. B. C. Gates, L. Guczi and H. Knözinger, Elsevier, Amsterdam, 1986; *Tailored Metal Catalysts*, ed. Y. Iwasawa, Reidel, Dordrecht, 1986.

2 K. Asakura, K. Bando and Y. Iwasawa, *J. Chem. Soc., Faraday Trans.*, 1990, 2645.

3 J. Evans and G. S. McNulty, *J. Chem. Soc., Dalton Trans.*, 1984, 1123.

4 K. Asakura and Y. Iwasawa, *J. Chem. Soc., Faraday Trans.* 1990, 2657.

5 P. S. Kirlin, F. B. M. van Zon, D. C. Koningsberger and B. C. Gates, *J. Phys. Chem.*, 1990, **94**, 8439.

6 P. S. Kirlin, H. Knözinger and B. C. Gates, *J. Phys. Chem.*, 1990, **94**, 8451.

7 T. Chihara, K. Aoki and H. Yamazaki, *J. Organomet. Chem.*, 1990, **383**, 367.

8 Y. Izumi, T. Liu, K. Asakura, T. Chihara, H. Yamazaki and Y. Iwasawa, *J. Chem. Soc., Dalton Trans.*, 1992, 2287.

9 T. Chihara and H. Yamazaki, unpublished work.

10 F. Calderazzo, *Angew. Chem., Int. Ed. Engl.*, 1977, **16**, 299.

11 S. C. Wright and M. C. Baird, *J. Am. Chem. Soc.*, 1985, **107**, 6899.

12 A. Dedieu, S. Sakaki, A. Strich and P. E. M. Siegbahn, *Chem. Phys. Lett.*, 1987, **133**, 317.

13 N. Koga and K. Morokuma, *J. Am. Chem. Soc.*, 1985, **107**, 7230.

14 G. Pacchioni, P. Fantucci, J. Koutecký and V. Ponec, *J. Catal.*, 1988, **112**, 34.

15 G. Huttner, J. Schneider, H. Müller, G. Mohr, J. Seyerl and L. Wohlfahrt, *Angew. Chem., Int. Ed. Engl.*, 1979, **18**, 76.

16 R. Ryan, C. U. Pittman, jun. and J. P. O'Connor, *J. Am. Chem. Soc.*, 1977, **99**, 1986.

17 E. L. Muetterties and M. J. Krause, *Angew. Chem., Int. Ed. Engl.*, 1983, **22**, 135.

18 G. Süss-Fink and G. Hermann, *J. Chem. Soc., Chem. Commun.*, 1985, 735.

19 Y. Izumi, T. Chihara, H. Yamazaki and Y. Iwasawa, *J. Chem. Soc., Chem. Commun.*, 1992, 1395.

Received 29*th July* 1993; *Paper* 3/04555B